Vapor-liquid-solid nucleation of GaAs on Si(111): Growth evolution from traces to nanowires

S. Breuer,* M. Hilse, A. Trampert, L. Geelhaar, and H. Riechert
Paul-Drude-Institut für Festkörperelektronik, Hausvogteiplatz 5-7, 10117 Berlin, Germany
(Received 25 February 2010; revised manuscript received 16 July 2010; published 6 August 2010)

GaAs nanowires were grown on Si(111) substrates by molecular-beam epitaxy employing Au droplets for the vapor-liquid-solid mechanism. The nucleation happens in three stages, which coincide with the abundance of one of three different GaAs manifestations: first Au-induced lateral traces, then three-dimensional islands, and finally Au-induced vertical nanowires. During deposition of the first 7 ML of GaAs no nanowires grew. By reflection high-energy electron diffraction and transmission electron microscopy, the crystal structure of the GaAs manifestations was examined. Traces and islands adopted the zinc-blende crystal structure and include twins, while nanowires grew in the hexagonal wurtzite structure. The delay in nanowire formation was observed to increase for higher growth temperatures. The gradual covering of the Si by GaAs was comparable to the case of Au-free growth and appears to be linked with the evolution from trace to nanowire growth. During trace formation, Au droplets kept in contact with the Si substrate and were pushed sideways by precipitating GaAs. The nucleation stages could thus be explained by considering that any Au droplet created a trace while in contact with the Si surface and a nanowire after having been pushed onto GaAs. This mechanism of trace growth was explained by the lower interface energy of liquid Au droplets on Si when compared with that on GaAs, as supported by numerical estimates.

DOI: 10.1103/PhysRevB.82.075406 PACS number(s): 81.10.Aj, 62.23.Hj, 68.65.−k, 68.08.−p

I. INTRODUCTION

Semiconductor nanowires (NWs) are considered as promising building blocks for various nanosized devices.[1] One particular advantage of the NW geometry arises wherever heterointerfaces are involved. In planar heterostructures, the adsorbate crystal quality may be limited by defects generated to accommodate the structural differences between the two involved materials. In contrast, axial heterostructures within nanowires or between vertical nanowires and the substrate are believed to overcome many of these inhibitions. Since the interface between the two different materials is very small, strain induced by lattice mismatch can elastically relax at the nearby free sidewalls. Consequently, the critical thickness at which dislocations form is larger than for planar heterostructures.[2,3] A prominent example for the importance of this advantage is the ongoing effort to integrate compound semiconductors with Si with the aim of combining the direct band gap and high electron mobility of the former with the mature technology of the latter.[4]

GaAs is arguably the most intensively studied compound semiconductor, and thus its heteroepitaxy on Si can be considered as a role model for monolithic integration.[5] The strong dissimilarity of GaAs and Si, viz., 4% lattice mismatch and 55% mismatch in the thermal-expansion coefficients usually produces threading dislocations with a density as high as 10^9-10^{10} cm^{-2}. By thermal cycling and inserting buffer layers, this value can be reduced but the minimum density to date[6] remains $\sim 10^6$ cm^{-2}. Obviously, in any heteroepitaxy the nucleation phase is critical for the crystal quality of the whole layer. During the growth of the first few monolayers (MLs) the mutual interaction of the two materials is most intense and the structural details of the first few MLs strongly influence the quality of the following growth. Due to the energetic preference of the Si substrate surface, the nucleation of GaAs on Si follows the Volmer-Weber mechanism and proceeds by forming three-dimensional (3D) islands. At the very initial stage of growth, the height of a GaAs/Si island relates to its lateral size as $h/l=1/2$. As growth progresses beyond a critical thickness [$\sim$4 ML on Si(001) (Ref. 7)], dislocations nucleate in higher stress regions near island edges by way of which the islands partially relax. These dislocated islands approximately retain their hemispherical shape during further growth until eventual coalescence leads to the high density of threading dislocations in the thick epitaxial layer.

The growth of GaAs on Si substrates in the form of nanowires has been demonstrated both by metal-organic vapor phase epitaxy (MOVPE) [Refs. 8–11] and by molecular-beam epitaxy (MBE).[12–14] In all these cases, the formation of nanowires was induced by Au droplets in the framework of the vapor-liquid-solid (VLS) growth mechanism,[15] which has recently been reviewed and expanded.[16] Only very recently, GaAs nanowires were grown on Si without Au but by using an unpatterned thin SiO_x layer.[17,18] However, in none of all these reports the crystal quality of the GaAs NWs at the interface region was addressed, and no special attention was paid to the nucleation phase.

In this study, we investigate in detail the nucleation of Au-induced GaAs nanowires grown by MBE on Si(111). We observe that the formation of nanowires is delayed. Initially, quasi-one-dimensional laterally elongated GaAs structures termed "traces" grow, followed by 3D islands. Only after the whole Si substrate is thus covered by GaAs, the traces evolve to form vertical, strain-free nanowires. Similar to the Au-free nucleation of GaAs on Si as islands, lower growth temperatures accelerate the formation of a closed GaAs layer which results in faster vertical nanowire formation. The evolution process is explained by differences in interface energies.

II. NUCLEATION STUDY

Quartered two-inch, *n*-type, Si(111) $\pm 0.5°$ substrates were loaded into the MBE system. After water desorption at

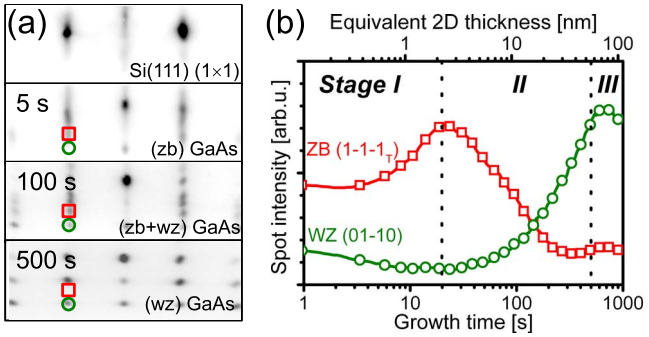

FIG. 1. (Color online) (a) Four RHEED patterns showing: the (1×1) As-terminated Si(111) surface before growth, the pattern of ZB GaAs with twins after 5 s, the superposition of ZB and WZ GaAs after 100 s, and the WZ GaAs diffraction pattern after 500 s which remains unchanged until growth ends. (b) The time-dependent intensities of a ZB and a WZ spot give evidence for a gradual change from nucleation in the ZB to growth in the WZ crystal structure. The resulting three growth stages are indicated. The two analyzed spots are marked in (a): ZB $(1\bar{1}\bar{1})_T$ by squares and WZ $(01\bar{1}0)$ by circles.

300 °C, the silicon oxide was removed from the substrates by Ga polishing, viz., deposition of 3 nm Ga at a substrate temperature of 500 °C followed by GaO_x desorption at 800 °C and formation of Si(111) terraces.[19] Au droplets were prepared on the clean surface by depositing ≈0.6 nm Au at 400 °C and annealing at 550 °C for 5 min. The diameter of the droplets varied between 2 and 20 nm. For nanowire growth, the substrate temperature was set to 500 °C. The As valve was opened before growth to establish a stable As supply. The Ga shutter opening initiated GaAs growth. The V/III flux ratio, i.e., F_{As}/F_{Ga}, was set to 2.0 and the Ga flux was set to match a planar GaAs(111)B growth rate of 0.11 nm/s; the Ga and As fluxes were calibrated using reflection high-energy electron-diffraction (RHEED) oscillations on GaAs(001) substrates.

A. RHEED—Zinc blende to wurtzite evolution

Two distinct GaAs structures could be expected to form during the nucleation: if nucleation followed the Volmer-Weber mechanism as in the Au-free planar case then 3D islands would be expected. Alternatively, if nucleation was dominated by the Au-assisted VLS growth, nanowires would appear immediately. In 3D islands, GaAs grows in the usual zinc-blende (ZB) crystal structure[5] but in Au-induced nanowires, GaAs often adopts the wurtzite (WZ) crystal structure.[12,20] Both can be discriminated *in situ* during MBE growth by RHEED.

GaAs nanowires were grown at 500 °C for 30 min, during which the total deposition was equivalent to a planar two-dimensional (2D) GaAs thickness of $d=200$ nm. The development of the crystal structure was studied during growth by RHEED with the incidence azimuth along $\langle 1\bar{1}0\rangle$, cf. Fig. 1(a). Prior to growth, the Si(111) reflection pattern without superstructure was observed, which is in agreement with the Si(111):As (1×1) surface expected to form in an As-containing MBE growth chamber.[21] After 5 s of growth, cubic ZB GaAs and its twin pattern were observed. Vertical discontinuities indicated the transmission through 3D structures. After 100 s, hexagonal WZ transmission spots had appeared in addition to the ZB pattern. After 500 s, only the WZ transmission diffraction pattern was observed. Afterwards, the RHEED pattern remained unchanged until the end of growth.

Toward a quantification of the crystal structure transition, one spot of each RHEED pattern was chosen for temporal intensity profiling, here the WZ $(01\bar{1}0)$ and ZB $(1\bar{1}\bar{1})_T$ spots, where the subscript T indicates the twin orientation. Figure 1(b) shows the resultant profiles. The intensity development can be divided into three stages: in stage I, from growth start until 20 s, exclusively the ZB spot intensity increased while the WZ spot intensity remained very low. During this stage, ≈2.2 nm of GaAs (equivalent 2D thickness) were grown. In stage II, from 20 s until 500 s, the intensity of the WZ phase increased while the ZB pattern gradually vanished. Obviously, the crystal structure of the growing material changed. In stage III, from 500 s until the end of growth, only WZ GaAs was detected.

Our investigation by RHEED showed that the dominating crystal structure evolved from ZB with twins to WZ. Supposing the ZB signal arose from GaAs island growth and the WZ signal from GaAs nanowires, a temporal delay in nanowire formation was deduced. In order to test this, growth was interrupted in a series of samples after different times and the morphology was analyzed.

B. Growth time series—From traces to nanowires

The growth time series was performed at 500 °C substrate temperature. Samples were grown for 5, 60, 300, and 1800 s and their morphology was characterized by scanning electron microscopy (SEM) in 45° incidence, cf. Fig. 2(a). The contrast was adjusted such that Si is shown in black and GaAs in gray.

After 5 s, the total GaAs deposition was equivalent to a 2D thickness of $d=0.6$ nm. Instead of nanowires or islands, GaAs had formed a high number of long and curved structures with a bright contrast droplet at one end each. Since these structures look like they were created by moving droplets, they are called traces.

After 60 s, $d=6.6$ nm, in addition to traces many larger structures were present. Islands were distinguished from traces by the absence of the bright features at their ends and by their larger height. Many islands were elongated along one in-plane direction and the majority was connected to traces and other islands. Furthermore, a small number of vertical structures in very bright contrast was present, identified as the first nanowires.

After 300 s, $d=33$ nm, traces were not observed anymore. Instead, there were many islands whose size had increased and several of which had coalesced. Also, the nanowires had increased in number and length and their position was unambiguously on the GaAs islands.

After 1800 s, $d=200$ nm, only nanowires and at their base a rough layer of continuous GaAs were present. The

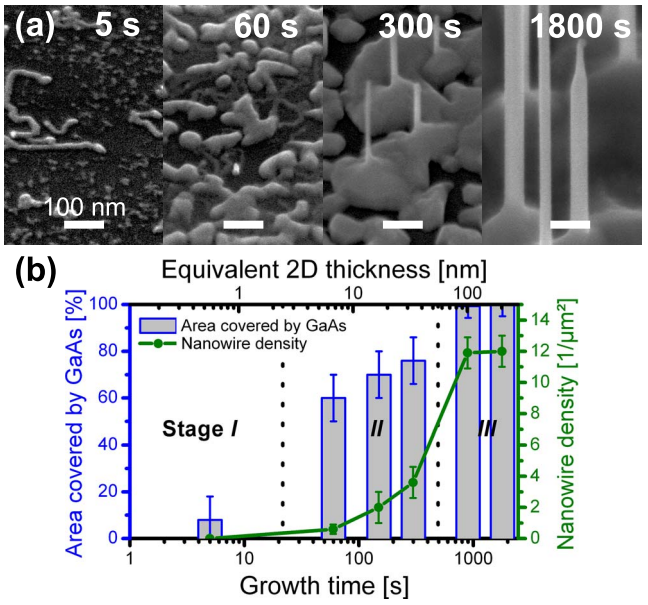

FIG. 2. (Color online) (a) SEM images in 45° incidence of samples grown at 500 °C for different durations. All scale bars indicate 100 nm. The following GaAs structures were identified: traces after 5 s, traces and islands after 60 s, islands and nanowires after 300 s, and nanowires on a coalesced layer after 1800 s. (b) The plot shows the percentage of the Si surface area covered by GaAs and the number density of nanowires versus growth time. The three stages are indicated.

density of the nanowires had further increased, equally so their diameter and length. The thickness of the basal GaAs layer was ≈100 nm.

Additional normal-incidence SEM images were used for quantitative analysis. The nanowires were counted and α_{GaAs}, the area percentage covered by GaAs, was calculated. The results for α_{GaAs} and the nanowire density are presented in Fig. 2(b) where the three RHEED-determined growth stages are also indicated. Phases I, II, and III coincide with none, intermediate, and saturated nanowire density as well as low, intermediate, and full GaAs covering, respectively. In particular, the temporal development of the nanowire density in Fig. 2(b) closely resembles that of the WZ RHEED intensity presented in Fig. 1(b), which is in agreement with the WZ crystal structure of nanowires (also see below).

The growth time study shows that nucleation starts by the initial formation of traces (stage I), then an intermediate phase during which islands dominate (stage II), and only in the long run nanowire growth prevails (stage III). This sequence coincides exactly with the three stages that were determined by the RHEED analysis of the ZB and the WZ crystal structure intensities.

In stage I, traces of different sizes dominate the growth and are identified as the 3D structures with ZB crystal structure observed by RHEED. The majority of GaAs grew in the form of larger traces, in between which there are smaller structures which are probably small GaAs traces. Possibly, all GaAs nucleated on Si in the form of traces that were induced by Au droplets. However, the additional formation of few very small islands by the Volmer-Weber mechanism cannot be excluded.

During stage II, the number of traces decreases while the number of nanowires increases but most GaAs grows in the form of islands. The appearance of islands demonstrates that GaAs can grow without Au droplets by direct attachment of the growth species from the vapor phase onto any solid GaAs structures, leading to lateral and vertical growth. The shape of many islands indicates that they may originate from GaAs trace tails. The gradual covering of the Si substrate by GaAs is made up by two contributions: direct attachment to traces, islands, and eventually nanowire bases as well as ongoing trace growth by the VLS mechanism.

Stage III starts when all GaAs structures coalesced and the Si surface is completely covered by a continuous GaAs layer. From this moment on, the nanowire density is maximal and stays constant. Further growth leads to an increasing length and diameter of the nanowires, an increasing size of a pyramidal base at the lower part of every nanowire, and an increasing thickness of the planar GaAs layer between the nanowires. Growth thus closely resembles the Au-induced homoepitaxy of GaAs nanowires on GaAs(111)B substrates.[22]

A similar trace to nanowire evolution was recently reported in MOVPE studies of the Au-induced nucleation of InAs nanowires on GaAs substrates.[23,24] In that system there was no growth of islands. Initially, droplets led to trace growth, and where the Au droplet of one trace front met the InAs tail of another trace its lateral motion stopped and vertical nanowires formed. Furthermore, on SEM images of InAs/GaP axial nanowire heterostructures in the supporting information of Dick *et al.*,[10] traces can clearly be seen on the substrate.

C. High-resolution TEM—Traces on Si, nanowires on GaAs

High-resolution transmission electron microscopy (HRTEM) was performed to study the GaAs manifestations in detail and to locally resolve the overall crystal structure evolution as determined by RHEED. To both ends, HRTEM micrographs were recorded at different regions on the same sample grown for 150 s (d=17 nm) on which traces, islands, and nanowires coexist. These micrographs and local Fourier transforms are shown in Fig. 3.

In an overview TEM image [Fig. 3(a)], a typical trace is displayed in its entirety. A magnification of its frontal region is shown in Fig. 3(b). The trace has the ZB crystal structure and exhibits twins. There is clearly a crystallized Au droplet at one end. The Au droplet exhibits one interface each to the Si substrate and to the GaAs trace. The height of the GaAs trace is comparable to the droplet diameter.

A typical island is presented in Fig. 3(c). The GaAs grew in the ZB structure. Stacking faults and nanotwins can be observed, most eminently close to the substrate.

In Fig. 3(d) a typical nanowire is shown. All analyzed nanowires indeed display the WZ crystal structure and one Au droplet located at their tip. Between the WZ GaAs nanowire and the Si substrate there is a base of ZB GaAs. This base structurally closely resembles traces and islands in that there are many stacking faults. The Au droplet diameter matches the nanowire diameter, typically 5 nm. This particu-

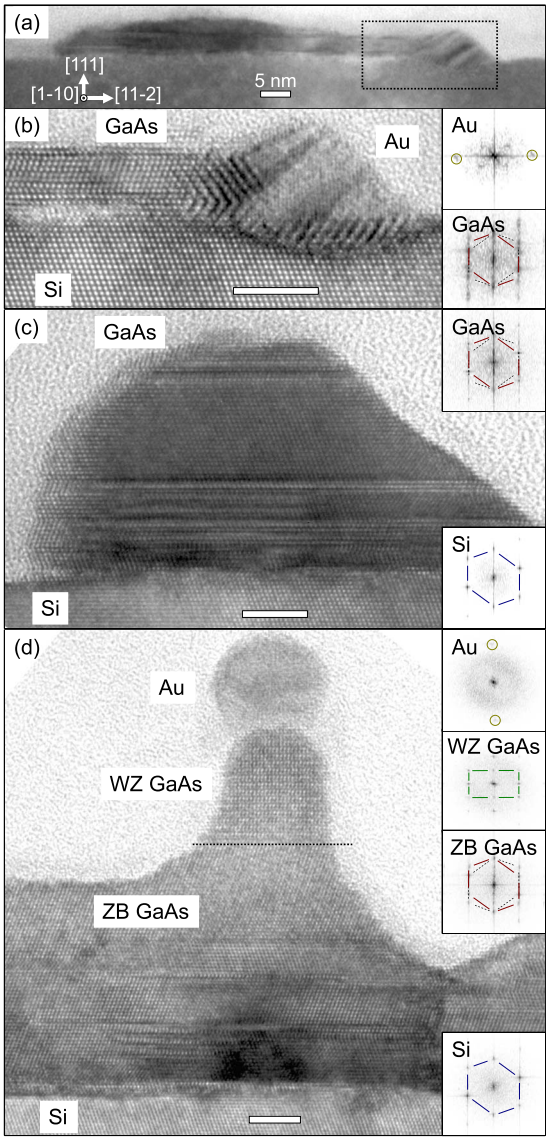

FIG. 3. (Color online) TEM micrographs at different regions of the same sample grown for 150 s at 500 °C: (a) GaAs trace with frontal Au droplet; (b) same trace in high resolution showing the ZB crystal structure with twins and the crystallized Au droplet; (c) 3D GaAs island, structurally ZB with twins; and (d) WZ GaAs nanowire with Au droplet at the tip and a ZB GaAs base layer. All scale bars indicate 5 nm. The insets show 2D Fourier transformations of selected regions for their crystal structure identification.

lar nanowire is 10 nm long, as measured over the WZ segment and the ZB region below is 22 nm high.

The HRTEM investigation confirms the earlier assignments in crystal structure of WZ to nanowires and ZB with twinning to traces and islands. In this way, the evolution in the RHEED-detected crystal structures from ZB to WZ matches the SEM-determined evolution from traces and islands to nanowires. Furthermore, both traces and nanowires indeed form by VLS growth from Au droplets. While traces have direct contact to Si, nanowires stand on a base of GaAs. The evolution from trace to nanowire growth may thus depend on the two underlying surfaces.

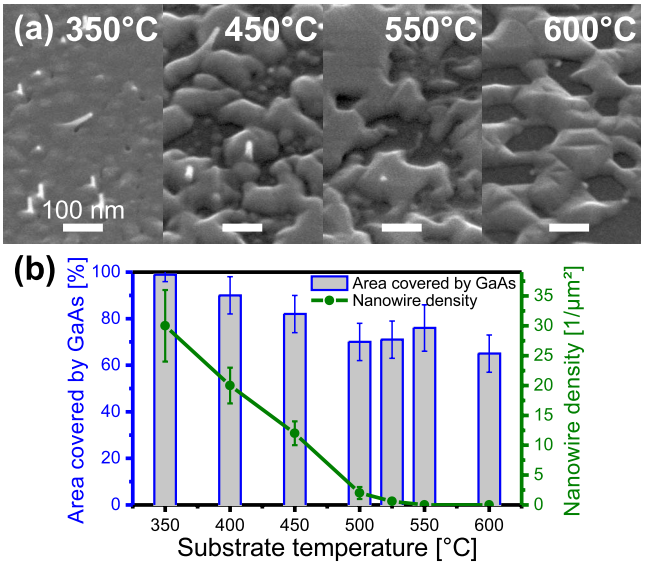

FIG. 4. (Color online) (a) SEM images in 45° incidence of samples grown for 150 s at various substrate temperatures: at 350 °C the Si substrate was covered by GaAs and many nanowires grew; at 450 °C GaAs had formed islands, traces on remaining Si and nanowires on the GaAs islands; at 550 °C island growth was confined to a smaller total area, many traces grew, and nanowires did not form; and at 600 °C only islands grew. (b) Plot of the temperature dependence of the area covered by GaAs and the nanowire density. Both show an essentially parallel trend with temperature.

D. Temperature series–Suppressed diffusion accelerates evolution

In order to obtain further insight into the nucleation mechanisms, a series of samples was grown for 150 s (d =16.5 nm) at different substrate temperatures. Figure 4(a) shows 45° incidence SEM images of the samples grown at T_S=350, 450, 550, and 600 °C. At 350 °C the substrate was almost completely covered by GaAs that had already coalesced to a rough layer. Nanowires were present in between and no traces were seen. On the sample grown at 450 °C, there were fewer nanowires and some traces. GaAs coalescence and coverage of Si were less complete. At 550 °C, even more traces and free Si surface but less area covered by GaAs was present. Nanowires were few and short. The sample grown at 600 °C showed the smallest covered surface fraction of the study. There were neither nanowires nor traces.

As before, normal-incidence SEM images of these samples were analyzed quantitatively and the results are shown in Fig. 4(b). With increasing temperature, α_{GaAs} exhibits an essentially decreasing trend. This reproduces the Au-free case,[25] in which a lower T_S effectively suppresses the kinetics of island formation by reduced Ga diffusion, and GaAs tends to grow as a closed layer. With increasing T_S from 350 to 525 °C, the nanowire density decreases approximately in parallel with α_{GaAs}. This means that the nanowire density is lower when the total GaAs coverage is lower, similar to the growth time series discussed earlier, which provides further evidence that nanowires form in connection

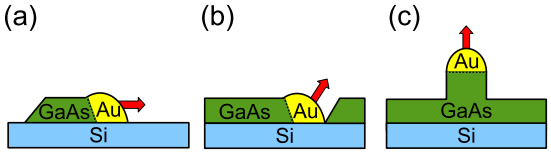

FIG. 5. (Color online) Schematic of (a) trace growth, (b) transition from trace to nanowire growth, and (c) nanowire growth. While the GaAs growth front is at the droplet-GaAs interface, the droplet-Si interface has a lower interface energy. The resulting growth directions are indicated by arrows.

with GaAs-covered areas. In the range from 500 to 550 °C, an increasing number of traces could be identified while nanowires were increasingly scarce. Possibly, trace growth is the origin of the rising slope of α_{GaAs} in this temperature range. On the sample grown at 600 °C neither nanowires nor traces are visible, which indicates that growth by the VLS mechanism did not take place. This compares well with homoepitaxial GaAs nanowire growth on GaAs(111)B, where nanowire growth stops above 620 °C.[22]

These observations show that the transition time of VLS growth from pure trace formation (stage I) to pure nanowire formation (stage III) depends on growth temperature and increases with temperature. For all temperatures below 600 °C, nanowires grew on GaAs while traces grew on Si.

III. EVOLUTION MODEL

What determines the evolution of the GaAs growth in stages from traces to nanowires? Both trace fronts and nanowires grow from Au droplets by the VLS mechanism, while in parallel direct epitaxial attachment first leads to the growth of trace ends to islands and possibly Volmer-Weber island nuclei, then adds to the coalescence of all GaAs structures, and finally governs the growth of the basal layer between the nanowires. As a result, initially traces grow on Si and later nanowires grow on GaAs. For an understanding of the VLS growth evolution, the influence of the liquid-solid interface must be clarified.

In a nanowire, the droplet completely adjoins GaAs and further growth adds material to this interface, cf. Fig. 5(c). This is different in a trace, cf. Fig. 5(a). Here, the droplet adjoins GaAs as well as Si and while further growth of GaAs from the droplet adds material homoepitaxially at the GaAs interface, the experimental data suggest that it is favorable for the droplet to keep the Si interface area constant by lateral motion. Thus, from the initial prevalence of traces, a smaller interface energy of the Au/Si can be concluded as compared to Au/GaAs,

$$\sigma_{ls}^{\mathrm{Au/Si}} < \sigma_{ls}^{\mathrm{Au/GaAs}}. \tag{1}$$

In order to verify this, the energies of the two competing liquid-solid interfaces are estimated. In the present system, various experimental as well as theoretical studies allow the calculation of the interface energies by Young's equation,

$$\sigma_{sv} = \sigma_{lv}\cos(\alpha) + \sigma_{ls}, \tag{2}$$

where α is the contact angle measured inside the droplet and σ_{sv}, σ_{lv}, and σ_{ls} are the solid-vapor, liquid-vapor, and liquid-solid interface energies, respectively.

To be precise, the liquid Au droplet accumulates Ga during growth and the resultant alloy has been shown to contain up to 50% Ga (stoichiometric AuGa) in an analysis of GaAs nanowires on the homoepitaxial substrate.[26] An estimation of σ_{ls} can thus be made using the experimental values[27] for $\sigma_{lv}(\mathrm{Au})=71$ meV/Å^2 and $\sigma_{lv}(\mathrm{Ga})=45$ meV/Å^2, and interpolating to a Ga content of 50%.

The interface energy of Si(111) has been measured[28] to $\sigma_{sv}=77$ meV/Å^2, which is considered as an upper limit since theoretical calculations demonstrate that the Si(111) surface energy is substantially lowered by the As termination that arises in the As-rich growth conditions used.[29] The contact angle of liquid Au on Si(111) is $\alpha=43°$, which has been experimentally determined[30] and also corresponds to the angle visible in Fig. 3(b). This yields an estimate of $\sigma_{ls}^{\mathrm{AuGa/Si}} \leq 35$ meV/Å^2 for stoichiometric AuGa and an even lower ≤ 25 meV/Å^2 for pure Au.

For the GaAs interface energy, we consider the calculated[31] lowest energy surface under As-rich conditions which is (111)B reconstructed with As trimers and has $\sigma_{sv}=43$ meV/Å^2. The contact angle of liquid Au on GaAs(111)B has been measured on nanowire samples[20] to lie between 90° and 125°. The difficulty of measuring contact angles at nanowires is due to the curvature of the underlying GaAs as apparent in Fig. 3. Thus the interface energy of the liquid droplet on GaAs(111)B is estimated as $\sigma_{ls}^{\mathrm{AuGa/GaAs}} \geq 43$ meV/Å^2 and the same value for pure Au as in accordance with Glas *et al.*[20] From these estimations we conclude that the interface energy of liquid droplets is indeed lower on Si(111) than on GaAs(111)B, which supports the trace formation mechanism described above.

These findings can be used to elucidate the observed consecutive growth stages. The initial prevalence of traces has been explained by a lower droplet interface energy on Si(111), which is initially exposed (stage I), cf. Fig. 5(a). In the process of VLS trace and non-VLS island growth, GaAs gradually covers the Si substrate.

Eventually, no more Si is available in the neighborhood of a particular AuGa droplet so that it cannot continue trace growth, cf. Fig. 5(b). This triggers the turnover from horizontal trace to vertical nanowire growth since the driving force for lateral motion has vanished. The last Si remaining directly under the droplet is covered either by further lateral growth of the GaAs trace front or by GaAs nucleating at the Si interface. In both cases, the droplet is pushed upward in the process.

From this point on, the liquid-solid interface of the droplet is completely made up of AuGa/GaAs. This interface is again the location of GaAs precipitation but there is no more energy gain from lateral motion. Instead, the nanowire is pushed vertically upward by its own precipitate, cf. Fig. 5(c). As soon as the AuGa/GaAs interface has risen above the neighboring GaAs structures, vertical sidewalls can be formed and the vertically growing GaAs nanowire is then expected to adopt the WZ crystal structure.[20] At a later stage however, lower parts of the nanowire may switch to ZB, when neighboring ZB structures encompass the bottom of the nanowire.[32] This structural switch can explain why the nanowire shown in Fig. 3(d) is WZ only above the level at which vertical sidewalls begin. We thus expect that the re-

gion directly below this WZ segment has also been formed by VLS nanowire growth and that at least a part of this region originally adopted the WZ structure but later switched to ZB, when it was enclosed by neighboring GaAs.

Due to the random positions of the AuGa droplets not all switch from trace to nanowire growth simultaneously. Stage II consists of the transition period that starts when the first droplet switched and ends when the last one did, i.e., when the Si is completely covered by GaAs. From then on, nucleation is finished and nanowires grow identical to the homoepitaxial case (stage III).

Due to the scarcity in nanowire nucleation studies, our findings can at present only be compared with the MOVPE growth of an axial heterostructure of GaAs on Si *within* nanowires studied by Dick *et al.*[10] Straight heterostructures of GaAs on Si nanowires were observed and explained by wetting of the Si nanowire base segment by the GaAs nanowire top segment and implicitly also by the Au droplet. This does not seem to correspond to the present situation, where GaAs on Si does not readily nucleate as a straight vertical nanowire. However, it also does not correspond to planar heterogrowth of GaAs on Si, which is nonwetting as represented by Volmer-Weber growth. It seems that the wetting situation is different in the three possible heterostructure combinations planar-planar, nanowire-planar, and nanowire-nanowire. Reasons for this may be (a) the involvement or not of a liquid droplet and its composition, (b) kinetic effects, and (c) that interface energies depend to some extend on external parameters such as droplet composition and chemical potentials. As an example, the described reduction in surface energies of GaAs(111)B and Si(111) by As termination may not be actualized in MOVPE. Indeed, Dick *et al.*[10] themselves expect that the wetting behavior may change if the interface energies are similar, which is in agreement with our estimations. Also, trace growth appears to be sensitive to the proper cleaning of the substrate surface. In separate experiments, during which weak RHEED patterns prior to growth indicated that the substrate had not properly been cleaned, the traces were considerably shorter and nanowires started to form in large number prior to the coalescence of GaAs.

IV. SUMMARY

In the Au-induced VLS growth of GaAs on Si(111), nanowires started to grow only after the first ≈ 20 s (7 ML) and their number increased until ≈ 500 s. This nucleation delay was explained by the formation of horizontal traces which arise since the liquid Au droplets have a lower interface energy on Si than on GaAs. Further growth is then dominated by GaAs islands, which form from trace ends or possibly from Volmer-Weber nuclei, and finally by the vertical nanowires with additional growth of a base layer, formed by coalescence of all earlier GaAs structures. In brief, the Au-induced nanowires grew only on a layer of GaAs.

Although the nanowires grow defect free in the WZ structure, the delay in nanowire formation leads to the development of a base layer with twins and stacking faults, which may limit the quality of electrical contacts through the substrate. Furthermore, trace growth is disadvantageous since it inhibits effective position control of the nanowires. The identification of the different droplet interface energies as the origin of trace growth is expected to assist in finding appropriate conditions for direct GaAs nanowire nucleation on Si.

ACKNOWLEDGMENT

We thank Vladimir Kaganer, Frank Grosse, and Peter Kratzer for helpful discussions.

*steffen.breuer@pdi-berlin.de

[1] C. M. Lieber and Z. L. Wang, MRS Bull. **32**, 99 (2007).
[2] F. Glas, Phys. Rev. B **74**, 121302(R) (2006).
[3] H. Ye, P. Lu, Z. Yu, Y. Song, D. Wang, and S. Wang, Nano Lett. **9**, 1921 (2009).
[4] E. P. A. M. Bakkers, M. T. Borgstrom, and M. A. Verheijen, MRS Bull. **32**, 117 (2007).
[5] Y. B. Bolkhovityanov and O. P. Pchelyakov, Phys. Usp. **51**, 437 (2008).
[6] W.-Y. Uen, Z.-Y. Li, Y.-C. Huang, M.-C. Chen, T.-N. Yang, S.-M. Lan, C.-H. Wu, H.-F. Hong, and G.-C. Chi, J. Cryst. Growth **295**, 103 (2006).
[7] H. Usui, H. Yasuda, and H. Mori, Appl. Phys. Lett. **89**, 173127 (2006).
[8] T. Mårtensson, C. Svensson, B. Wacaser, M. Larsson, W. Seifert, K. Deppert, A. Gustafsson, L. Wallenberg, and L. Samuelson, Nano Lett. **4**, 1987 (2004).
[9] A. Roest, M. Verheijen, O. Wunnicke, S. Serafin, H. Wondergem, and E. Bakkers, Nanotechnology **17**, S271 (2006).
[10] K. A. Dick, S. Kodambaka, M. C. Reuter, K. Deppert, L. Samuelson, W. Seifert, L. R. Wallenberg, and F. M. Ross, Nano Lett. **7**, 1817 (2007).
[11] X.-Y. Bao, C. Soci, D. Susac, J. Bratvold, D. P. R. Aplin, W. Wei, C.-Y. Chen, S. A. Dayeh, K. L. Kavanagh, and D. Wang, Nano Lett. **8**, 3755 (2008).
[12] I. P. Soshnikov, G. E. Cirlin, A. A. Tonkikh, V. N. Nevedomskii, Y. B. Samsonenko, and V. M. Ustinov, Phys. Solid State **49**, 1440 (2007).
[13] S.-G. Ihn, J.-I. Song, T.-W. Kim, D.-S. Leem, T. Lee, S.-G. Lee, E. K. Koh, and K. Song, Nano Lett. **7**, 39 (2007).
[14] J. H. Paek, T. Nishiwaki, M. Yamaguchi, and N. Sawaki, Phys. Status Solidi C **5**, 2740 (2008).
[15] R. S. Wagner and W. C. Ellis, Appl. Phys. Lett. **4**, 89 (1964).
[16] B. A. Wacaser, K. A. Dick, J. Johansson, M. T. Borgstrom, K. Deppert, and L. Samuelson, Adv. Mater. **21**, 153 (2009).
[17] F. Jabeen, V. Grillo, S. Rubini, and F. Martelli, Nanotechnology **19**, 275711 (2008).
[18] J. H. Paek, T. Nishiwaki, M. Yamaguchi, and N. Sawaki, Phys. Status Solidi C **6**, 1436 (2009).
[19] S. Wright and H. Kroemer, Appl. Phys. Lett. **36**, 210 (1980).
[20] F. Glas, J. C. Harmand, and G. Patriarche, Phys. Rev. Lett. **99**, 146101 (2007).

[21] R. I. G. Uhrberg, R. D. Bringans, M. A. Olmstead, R. Z. Bachrach, and J. E. Northrup, Phys. Rev. B **35**, 3945 (1987).
[22] J. C. Harmand, M. Tchernycheva, G. Patriarche, L. Travers, F. Glas, and G. Cirlin, J. Cryst. Growth **301-302**, 853 (2007).
[23] X. Zhang, J. Zou, M. Paladugu, Y. Guo, Y. Wang, Y. Kim, H. J. Joyce, Q. Gao, H. H. Tan, and C. Jagadish, Small **5**, 366 (2009).
[24] J. Bauer, U. Pietsch, A. Davydok, A. Biermanns, V. Gottschalch, and G. Wagner, Appl. Phys. A **96**, 851 (2009).
[25] D. K. Biegelsen, F. A. Ponce, A. J. Smith, and J. C. Tramontana, J. Appl. Phys. **61**, 1856 (1987).
[26] J. C. Harmand, G. Patriarche, N. Pere-Laperne, M.-N. Merat-Combes, L. Travers, and F. Glas, Appl. Phys. Lett. **87**, 203101 (2005).
[27] A. Zangwill, *Physics at Surfaces* (Cambridge University Press, Cambridge, England, 1988).
[28] D. J. Eaglesham, A. E. White, L. C. Feldman, N. Moriya, and D. C. Jacobson, Phys. Rev. Lett. **70**, 1643 (1993).
[29] D. K. Biegelsen, R. D. Bringans, J. E. Northrup, M. C. Schabel, and L.-E. Swartz, Phys. Rev. B **47**, 9589 (1993).
[30] B. Ressel, K. C. Prince, S. Heun, and Y. Homma, J. Appl. Phys. **93**, 3886 (2003).
[31] N. Moll, A. Kley, E. Pehlke, and M. Scheffler, Phys. Rev. B **54**, 8844 (1996).
[32] G. Patriarche, F. Glas, M. Tchernycheva, C. Sartel, L. Largeau, and J. C. Harmand, Nano Lett. **8**, 1638 (2008).